In vivo intracellular recording and perturbation of persistent activity in a neural integrator

E. Aksay[1,2], G. Gamkrelidze[1,2], H. S. Seung[1,3], R. Baker[2] and D. W. Tank[1]

[1] *Biological Computation Research Department, Bell Laboratories, Lucent Technologies, 700 Mountain Avenue, Murray Hill, New Jersey 07974, USA*

[2] *Department of Physiology and Neuroscience, New York University School of Medicine, New York, New York 10016, USA*

[3] *Howard Hughes Medical Institute, Brain and Cognitive Sciences Department, Massachusetts Institute of Technology, Cambridge, Massachusetts 02139, USA*

Correspondence should be addressed to D.W.T. (dwtank@lucent.com) or R.B. (bakerr01@endeavor.med.nyu.edu)

To investigate the mechanisms of persistent neural activity, we obtained *in vivo* intracellular recordings from neurons in an oculomotor neural integrator of the goldfish during spontaneous saccades and fixations. Persistent changes in firing rate following saccades were associated with step changes in interspike membrane potential that were correlated with changes in eye position. Perturbation of persistent activity with brief intracellular current pulses designed to mimic saccadic input only induced transient changes of firing rate and membrane potential. When neurons were hyperpolarized below action potential threshold, position-correlated step changes in membrane potential remained. Membrane potential fluctuations were greater during more depolarized steps. These results suggest that sustained changes in firing rate are supported not by either membrane multistability or changes in pacemaker currents, but rather by persistent changes in the rate or amplitude of synaptic inputs.

Persistent neural activity refers to a sustained change of sodium action potential firing rate extending beyond a brief sensory stimulus or motor command. This activity has been observed in diverse brain areas[1–8], suggesting that it is a general form of neural dynamics. Because persistent activity carries a 'trace' of a past event, it is thought to be closely related to short-term or 'working' memory[1,3,9]. In this study, we obtained intracellular recordings in awake goldfish from neurons that show sustained firing during eye fixation, providing information about intrinsic neuronal excitability and movement-associated membrane potential changes that constrains proposed mechanisms of persistent neural activity.

The neurons recorded are located in area I, a bilateral premotor hindbrain nucleus[7]. During sequential saccades and fixations composing the back and forth scanning pattern of goldfish spontaneous eye movements[10], these neurons discharge as shown in Fig. 1a (refs. 7, 11). Transient increases in firing rate are observed during ipsilaterally directed (on) saccades, and transient decreases occur during contralaterally directed (off) saccades. When eye position is above a threshold value, there is a sustained tonic firing rate that long outlasts the transient changes in rate observed during saccades (**Fig. 1b**). This persistent neural activity varies linearly with eye position, with different 'position' neurons showing different slopes and thresholds in the firing rate/eye position relationship[11].

This transformation of a pulse-like saccadic command into a step of sustained discharge can be described in terms of a velocity-to-position neural integrator (VPNI), a concept originally introduced[12] to explain the time integration of head-velocity signals into eye-position signals during the vestibulo-ocular reflex (VOR)[13]. Lidocaine inactivation of area I disrupts fixations and low-frequency VOR, demonstrating that this nucleus (connectivity, **Fig. 1c**) is an essential component of the VPNI for horizontal eye movements[7,11].

Hypothetical mechanisms for the persistent activity of VPNI position neurons must account for several characteristics[14]. First, there is a continuum of stable firing rates[5,6,11], which is more difficult to explain than bistability. Second, persistent activity remains without either visual[11] or proprioceptive feedback[15], demonstrating a central origin. Third, a different linear relationship between firing rate and eye position for each neuron implies that for each eye position, a constrained pattern of stable activity exists.

At one extreme, persistent activity may be a purely single-cell phenomenon. For example, burst input could trigger plateau potentials[16,17], with multiple dendritic generation sites producing multiple firing levels[18]. Alternatively, saccadic command neurons could release neuromodulators that modify the frequency of intrinsic pacemaker currents[19] or alter sodium action potential threshold[20] in a long-lasting way. At the other extreme, persistent neural activity may be produced by reverberatory activity in a positive feedback loop, a network mechanism explored in neural integrator models[14,21–24].

During intracellular recording from individual area I position neurons, we used current injection to perturb (stimulate or inhibit) with an artificial stimulus that produced a saccade-like transient change of activity. This provided a direct test for voltage-dependent regenerative events such as plateau potentials; simultaneously, it addressed whether a network of position neurons could integrate the increased firing rate of a single neuron. Intracellular recording was also used to reveal persistent step changes in interspike membrane potential associated with endogenous changes in firing rate and to investigate their origin. Finally, intra-

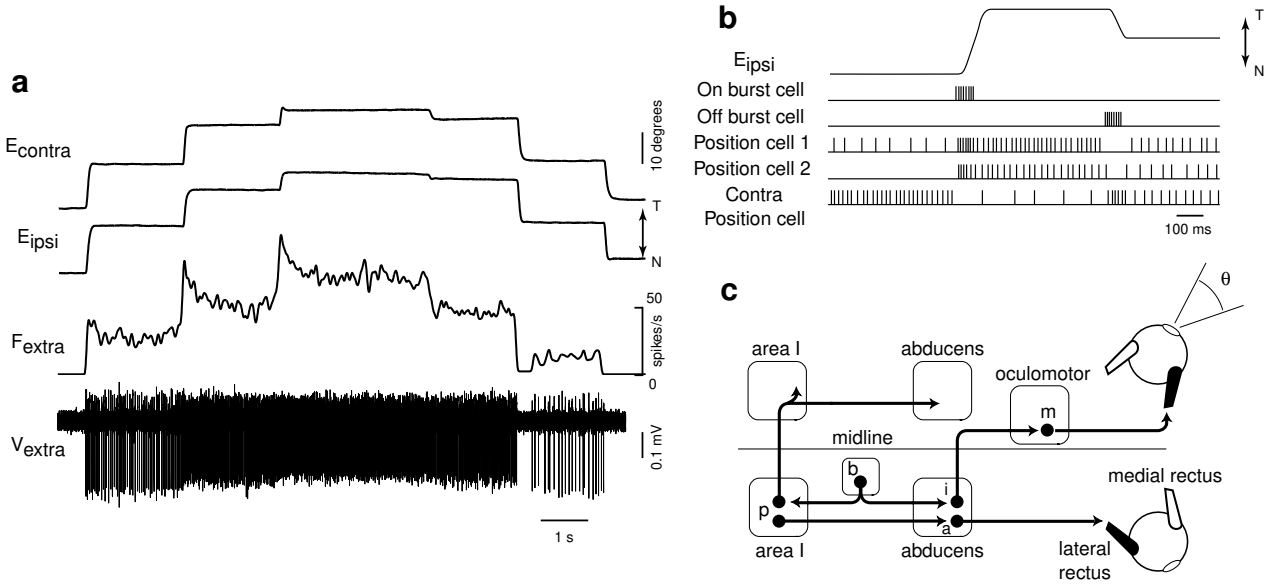

Fig. 1. Position neuron discharge and functional architecture of oculomotor pathways. (a) Extracellular voltage recording (V_{extra}) and firing rate (F_{extra}) of a position neuron in goldfish area I during one back and forth cycle of saccades and fixations (E_{ipsi}, ipsilateral eye; E_{contra}, contralateral eye; T, temporal; N, nasal). (b) Schematic showing eye position, burst neuron discharge and discharge of three position neurons during transitions in fixation position. On burst cell activity briefly precedes saccades and produces burst discharge of ipsilateral position neurons. This transient command is transformed into persistent elevated discharge of position neurons, supplying motoneurons with tonic drive necessary to maintain a new eye position. Off burst cell activity initiates saccades in the opposite direction and induces pauses in discharge followed by lowered persistent firing. Changes in firing rate are opposite in sign for contralateral position neurons. (c) Schematic of current understanding of functional connections underlying horizontal saccades and fixations. Saccades are initiated by burst neurons (b). Position neurons (p) in area I are required for the tonic discharge of abducens motoneurons (a) and medial rectus motoneurons (m; via internuclear cells, i) that determine the new eye position (θ). Each area I contains 30–50 position neurons, some of which may provide synaptic connections to the contralateral area I (ref. 11).

cellular recording allowed characterization of membrane potential fluctuations accompanying changes in persistent neural firing, thus addressing the role of synaptic activity.

Results

Spike discharge during intracellular recording

In vivo intracellular recordings were obtained from neurons in hindbrain area I of awake head-restrained goldfish performing scanning cycles of spontaneous saccades and fixations (**Fig. 1a**). Recordings from 18 position neurons were analyzed. Oculomotor behavior was quantified either directly by recording eye position (**Fig. 2a** and **b**), or indirectly by extracellular recording of a second position neuron in area I or a motoneuron in the abducens nucleus (**Fig. 2c**).

Intracellularly recorded position neurons (n = 18) injected with weak negative holding current (I_{inj}, 0 to –1 nA) discharged with qualitatively the same 'burst-tonic' pattern observed in extracellular recordings (**Fig. 1a**). On-direction steps in ipsilateral fixation position were accompanied by persistent increases in firing rate (**Fig. 2a** and **c**). Likewise, off-direction steps were accompanied by persistent decreases in rate (**Fig. 2b**). On-saccades were associated with brief (50–100 ms) bursts of discharge (**Fig. 2a** and **c**), whereas off-saccades were associated with brief (50–100 ms) undershoots in rate (**Fig. 2b**). Transitions between different persistent levels of firing were similar in amplitude (~5–50 spikes/s) to those recorded with extracellular electrodes[11].

The similarities in discharge pattern between recording methods suggest that position neurons functioned normally during intracellular recording. In addition, spontaneous sodium action potential width at half-maximum averaged 0.47 ± 0.16 ms (mean ± s.d.; n = 18), comparable to values seen for recordings with extracellular electrodes[11]. The population average for spontaneous action potential amplitude was 51 ± 14 mV (n = 18), and apparent resting membrane potential (mean over a scanning cycle) averaged –61 ± 7.3 mV (range, –70 to –50 mV; n = 8).

Position-associated membrane potential changes

Several forms of variation in current and/or conductance could explain the step-like changes of intracellular firing rate seen in Fig. 2. For example, the changes in tonic action potential frequency could be produced by changes in the frequency either of periodic synaptic currents that drive individual spikes[25] or of subthreshold oscillatory pacemaker currents[26]. Alternatively, the changes in firing rate could be produced by steady-state changes in membrane current or conductance that depolarize or hyperpolarize the spike generation zone. Interspike membrane potential (V_{is}) during discharge had step-like changes consistent with step-like changes in average current and/or conductance (**Fig. 2**). V_{is} was assessed by averaging sections of membrane potential after excluding action potentials (**Fig. 3a** and **b**). Transitions in rate associated with steps in fixation position were always accompanied by similarly directed transitions in the average value of V_{is}; increases in rate were coupled with increases (depolarizations) in potential (**Fig. 2a** and **c**; n = 18), and decreases in rate were accompanied by decreases (hyperpolarizations) in potential (**Fig. 2b**; n = 18).

This relationship between membrane potential and rate during spontaneous saccades and fixations was quantified for a com-

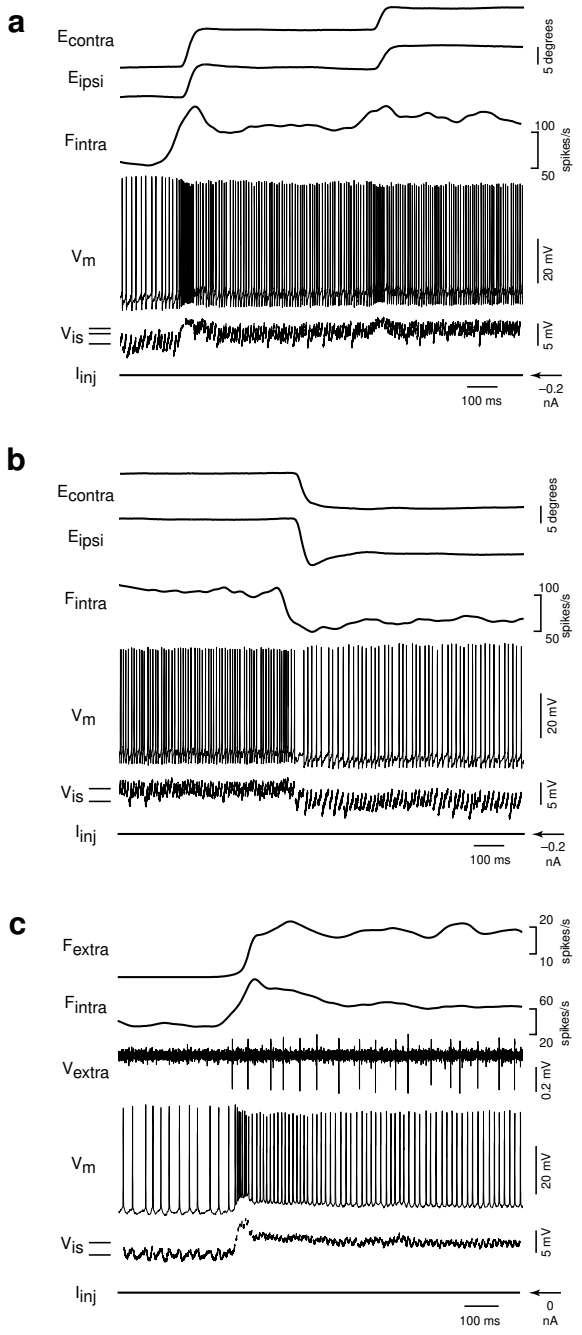

Fig. 2. Membrane potential changes during transitions in fixation position. (a) Eye position, firing rate of an intracellularly recorded neuron (F_{intra}), membrane potential (V_m), interspike membrane potential (V_{is}), and injected current (I_{inj}) for on-direction steps during intracellular recording. Solid lines at lower left indicate the average value of V_{is} during separate fixations. (b) Changes during off-direction steps of the ipsilateral eye. This segment is taken from the end of a nasal–temporal–nasal cycle that started with the transitions shown in (a). (c) Rate and potential changes for a different neuron during an on-direction step. The firing rate (F_{extra}) of a second extracellularly recorded position neuron (V_{extra}) served as a surrogate for eye position. In this recording, the fast afterhyperpolarization following action potentials was abolished by substituting cesium for potassium in the electrode solution.

plete cycle of the scanning pattern (4–10 fixations). Within one cycle, variation in mean V_{is} between nasal and temporal extremes averaged 4.7 ± 2.5 mV (n = 18), and could be as high as 10 mV. Firing rate increased with increasing V_{is}, with the highest rate and potential values at temporal fixations (**Fig. 3c** and **d**; n = 18). All correlation coefficients (r) for the rate–V_{is} relationship were greater than 0.7 (mean, 0.90; $p < 0.05$; n = 18). The slope (g_{spont}), a measure of the sensitivity of rate to fixation-related changes in mean potential, averaged 8.2 ± 5.6 spikes/s/mV (n = 18), ranging from 2.2 to 23 spikes/s/mV across recordings. In addition, V_{is} was correlated with fixation position, as assessed by eye position measurement (**Fig. 3e**; $r > 0.7$; mean, 0.87; $p < 0.05$; n = 3/3) and neuronal activity (**Fig. 3f**; $r > 0.80$; mean, 0.91; $p < 0.05$; n = 7/7).

If the steps in potential were indeed induced by steps in membrane current or conductance, then they should be present in the absence of action potential discharge. We tested this by hyperpolarizing with direct current injection through the recording electrode (n = 8). Addition of negative current resulted in hyperpolarization and reduced discharge rates at every fixation position (data not shown); strong negative current ($\Delta I_{inj} < 1.2$ nA, relative to original holding level) prevented the tonic discharge of action potentials altogether (**Fig. 4a** and **b**; n = 8/8). In the absence of action potentials, persistent changes in membrane potential (V_m) were still present, occurring in association with changes in fixation position (**Fig. 4a** and **b**; n = 8/8). During suppression of discharge, when quantified over a complete cycle of the scanning pattern, V_m was correlated with fixation position, as assessed by eye position measurement (**Fig. 4c**; r = 0.87, $p < 0.05$; n = 1/1) and neuronal activity (**Fig. 4d**; $r > 0.7$; mean, 0.90; $p < 0.05$; n = 5/5). Variation in mean V_m between nasal and temporal extremes averaged 3.7 ± 2.2 mV (n = 8), and could be as high as 10 mV.

The above results suggest that steps in membrane current and/or conductance producing persistent steps in average membrane potential contributed to fixation-related steps in firing rate. To determine if this contribution is sufficient, we compared the sensitivity of rate to variation in membrane potential for two distinct situations: when variation of rate and potential was associated with spontaneous saccades and fixations (sensitivity g_{spont}), and when variation was induced by current injection through the recording electrode (sensitivity g_{inj}). If sensitivity values were significantly less with electrode-generated change, this would cast doubt upon the sufficiency of membrane current changes in explaining the steps in rate. We calculated sensitivity g_{inj} as the slope of the relationship between firing rate and membrane potential changes induced by current steps or ramp-like current injection profiles applied during single fixations (**Fig. 5**; n = 12; see Methods). The population average for sensitivity g_{inj} was 12.3 ± 4.0 spikes/s/mV (n = 12), ranging from 6.8 to 20.0 spikes/s/mV, with an average error estimated to be ±20% due to bridge-balance imperfections. These sensitivity values always either matched or exceeded those determined from changes associated with spontaneous saccades and fixations: based on a cell-by-cell comparison, g_{inj} was 60.4 ± 15.1% higher than g_{spont} (n = 12). This result suggests that step-like changes in average membrane current polarizing the spike initiation zone would be sufficient to explain the fixation-related changes in rate.

We also tested whether a cell's sensitivity g_{spont} varied over the course of minutes. The relationship between firing rate and V_{is} was measured for five cycles of the scanning pattern done within a span of two minutes, as electrode holding current was fixed (I_{inj}, 0 to –1 nA; n = 3). The average sensitivities (± s.d.) for each cell were 4.9 ± 0.3, 7.1 ± 2.3 and 12.1 ± 1.6 spikes/s/mV. The small standard deviations in sensitivity suggest that the spike genera-

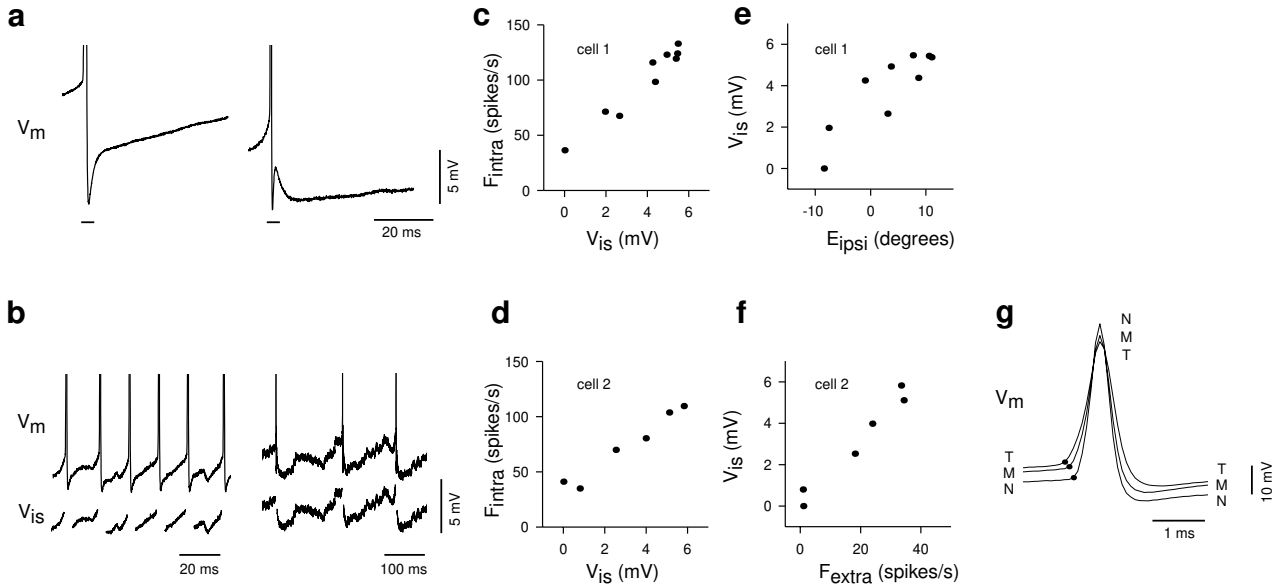

Fig. 3. Persistent change in firing rate and eye position correlated with persistent change in membrane potential. (**a**) Characteristic membrane potential during discharge. Average interspike membrane potential was assessed after excluding the underlined segments of data that began 1 ms before the peak of the action potential and ended 3 ms afterward. The data shown are averages of thirty action potentials taken from the same fixation; left and right panels are from two different neurons. (**b**) Membrane potential and interspike membrane potential remaining after spike exclusion for two position neurons. Right panels of (**a**) and (**b**) display data from the same cell. (**c**, **d**) Fixation-averaged intracellular firing rate plotted against fixation-averaged interspike membrane potential. The set of points in each figure correspond to the fixations made during one nasal–temporal–nasal scanning cycle, with membrane potential measured relative to the first fixation (cell 1, $r = 0.97$, $p < 0.001$, same cell as in **Fig. 2a** and **b**; cell 2, $r = 0.98$, $p < 0.001$, same cell as in **Fig. 2c**). (**e**) Interspike membrane potential plotted against eye position ($r = 0.86$, $p < 0.001$). (**f**) Interspike membrane potential plotted against the firing rate of a second extracellularly recorded position neuron ($r = 0.98$, $p < 0.001$). (**g**) Characteristic action potential waveform and threshold variation with fixation position (N, nasal position; M, mid-range position; T, temporal position; black dot, apparent action potential threshold).

tion mechanism for position neurons is largely constant on the minutes time scale during spontaneous saccades and fixations.

It has been proposed that slow, active conductances like the calcium-dependent potassium type may be involved in linearization of spike generation[27,28]. Position neuron action potentials displayed a prominent after-hyperpolarization (AHP) that was consistent with the presence of slow potassium conductances ($n = 15/18$, **Fig. 3a**). AHPs, assessed for action potentials followed by an interspike interval of at least 60 ms, were 2–10 mV deep, 20–40 ms in duration, and, in 3/15 recordings, displayed a distinct second minimum (**Fig. 3a**, right).

As previously presented, the suppression of action potential generation did not stop fixation-related steps in membrane potential (**Fig. 4**). However, AHPs and dendritic invasion could be important in modification of membrane currents and conductances, possibly influencing discharge rate. To explore this possibility, the relationship between potential and fixations over a complete scanning cycle was compared ($n = 5$) for the situations with discharge (**Fig. 3e** and **f**) and without discharge (**Fig. 4c** and **d**). Based on a paired *t*-test of the difference in slopes for cells where fixation behavior was monitored by neural recording, there was no significant change in sensitivity ($n = 5$, $p > 0.05$).

In addition to changes in spike frequency, variations in V_{is} were also associated with changes in spike shape. Action potentials simultaneously decreased in peak-to-peak amplitude (**Figs. 2** and **3g**) and increased in width at half-maximum (**Fig. 3g**) as V_{is}, firing rate and position increased; variation of spike amplitude with position was also seen with extracellular recordings[11] (**Fig. 1a**). Furthermore, the apparent threshold for action potential initiation, measured by determining the point on the spike rise where slope exceeded 15 mV/ms, was correlated with V_{is}, increasing with temporal positions (**Fig. 3g**; $r > 0.7$, $p < 0.05$; $n = 11/14$).

Visual inspection of recordings with action potentials suppressed by negative current injection revealed no indication of rhythmic oscillation in membrane potential (**Fig. 4a** and **b**; $n = 8/8$). Also, during low firing rates (<10 spikes/s), when the mean time between spikes exceeded the duration of spike AHP, V_{is} did not show evidence of an intrinsic rhythmicity (data not shown; $n = 18$). However, we observed non-rhythmic membrane potential fluctuations (analysis in final section of Results).

In addition to revealing steps in V_m, suppression of action potentials also exposed the presence of relatively large, transient (50–100 ms) depolarizations during on-saccades (**Fig. 4a**; $n = 7/8$). Deflections had peak potentials that were 2 to 14 mV above the subsequent post-saccadic potential ($n = 7/8$). The duration of these events closely matched the duration of bursts in firing rate seen at more depolarized levels (**Fig. 2a** and **c**) and during extracellular recording[11] (**Fig. 1a**; $n = 7/8$). During off-saccades in the absence of action potentials, membrane potential transitioned in a ramp-like fashion between two levels (**Fig. 4b**; $n = 8/8$). These transitions occurred typically in less than 100 ms, coinciding with the duration of undershoots in firing rate at more depolarized levels (**Fig. 2b**; $n = 8/8$).

The firing rate in the first 500 ms after the transient burst accompanying saccades frequently exhibited a slide toward a tonic level (**Fig. 2c**). This pattern of activity, possibly important in overcoming the visco-elastic properties of the oculomotor plant, has been previously observed in extracellular recordings of position

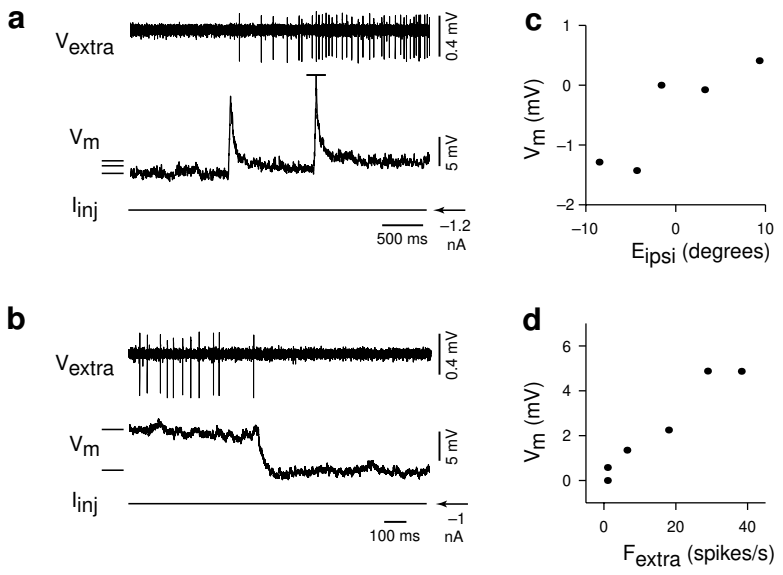

Fig. 4. Step-like changes in membrane potential in the presence of hyperpolarizing current. (**a**) Subthreshold, step-like depolarizations of membrane potential accompanying nasal to temporal steps of position during blockade of tonic activity with –1.2 nA of holding current. The second saccade elicited a single (truncated) action potential. (**b**) Subthreshold step hyperpolarization accompanying a temporal to nasal transition in position. (**c**) Fixation-averaged membrane potential plotted against eye position during suppression of discharge, with potential measured relative to the first fixation of the scanning cycle used (r = 0.87, p < 0.05). (**d**) Membrane potential for the cell in (**a**) plotted against the firing rate of a second extracellularly recorded position neuron (r = 0.97, p < 0.001).

neurons[11] (**Fig. 1a**). Associated with this slide in firing rate was slow relaxation of membrane potential, apparent at both depolarized (**Fig. 2c**) and hyperpolarized levels (**Fig. 4a**).

The results presented so far suggest that steps in membrane current and/or conductance that produced persistent steps in average membrane potential made a significant and possibly sufficient contribution to fixation-related steps of firing rate. The remainder of this study addresses how persistent steps in current and/or conductance might be generated and maintained in each position neuron.

Direct stimulation and transient change in activity

In principle, steps in membrane potential and firing rate could be the result of plateau potentials. These persistent events can be initiated with brief depolarizing current injections and stopped with brief hyperpolarizing injections through an intracellular recording electrode[29]. To investigate a possible involvement of regenerative plateau events in position neurons, we applied transient current injections in an effort to initiate and/or terminate persistent changes in discharge rate (n = 10). The presence of a persistent increase in rate following depolarizing steps or a persistent decrease following hyperpolarizing steps would be consistent with an involvement of plateau potentials. In addition, we used triangular current injections to see if position neurons showed hysteresis in their current–discharge relationship, another feature of cells with plateau potentials[16].

We maintained stable discharge activity (as in **Figs. 1a** and **2**) using weak holding current (I_{inj}, 0 to –1 nA). We assessed the firing rate before, during and after a given current injection within a single fixation. For depolarizing injections, stimulus duration was varied between 0.05 and 2.0 s; stimulus amplitude was varied between 0.3 and 3.0 nA. For hyperpolarizing injections, duration was varied between 0.1 s and 1.0 s; amplitude was varied between 0.5 and 1.0 nA.

When fixations were below a cell's position threshold, direct depolarizing injections were administered to elicit discharge rates of 30 to 300 spikes/s, matching, and in some neurons exceeding, the amplitude of firing rate bursts during on-saccades. All of these injections failed to result in after-discharge (**Fig. 5a**; n = 8/8). During stimulation, elevated firing rate after the first two interspike intervals either remained fixed or, particularly during large injections (> 1.0 nA), decayed slowly at rates of less than 10 spikes/s/s. Following rapid (< 0.1 ms) stimulus termination, averaged membrane potential returned to within 1 mV of the pre-stimulus level within 50 ms (n = 5/5).

When fixations were above a cell's position threshold, current stimulation also failed to result in after-discharge (**Fig. 5b**; n = 6/6). Firing rate during stimulation either remained fixed or decayed slowly (< 10 spikes/s/s). After stimulation, firing rate (F_{intra}) returned to a level similar to that before perturbation (–10 spikes/s < ΔF_{intra} < 5 spikes/s; weighted mean, –3.6 spikes/s; n = 6). The application of repeated steps in close succession failed to elicit any systematic increase in ΔF_{intra}.

Repeated depolarizing triangular current injections into one neuron were used to test for hysteresis in firing rate (n = 5 trials), but none was observed (**Fig. 5c** and **d**).

When fixations were above a cell's position threshold, negative current pulses were administered to suppress firing; all of these injections failed to generate persistent suppression of discharge (**Fig. 6a** and **b**; n = 3/3). After inhibition, firing rate returned to a level similar to that before perturbation (–10 spikes/s < ΔF_{intra} < 10 spikes/s; weighted mean, –2.1; n = 3/3); large-amplitude injections typically elicited a brief post-inhibitory rebound in discharge rate (**Fig. 6b**). The application of repeated steps in close succession failed to elicit any systematic decrease in ΔF_{intra}. Following rapid (< 0.1 ms) termination of injections applied below position threshold, averaged membrane potential returned, within 50 ms, to within 1 mV of the pre-stimulus level (n = 3/3).

We used repeated hyperpolarizing triangular current injections into one neuron during fixations below the position threshold to test for hysteresis in membrane potential (n = 5 trials), but none was observed (**Fig. 6c** and **d**).

For two recordings, cesium was substituted for potassium in the intracellular recording solution. Steps in membrane potential were still observed, even when the fast component of the AHP was eliminated (**Fig. 2c**). Under these conditions, with the electrotonic decay constant increased, brief current injections into one cell could not produce a sustained change in discharge rate (**Fig. 6b**).

The above results of direct stimulation constrain the role that voltage-dependent regenerative mechanisms could have in generation of the persistent firing exhibited by position neurons. Direct stimulation also allowed an estimation of apparent input impedance and relaxation time.

When neurons were at rest or slightly hyperpolarized (5–10 mV), apparent input impedance, quantified by applying small current steps (< 0.5 nA) in the absence of discharge, aver-

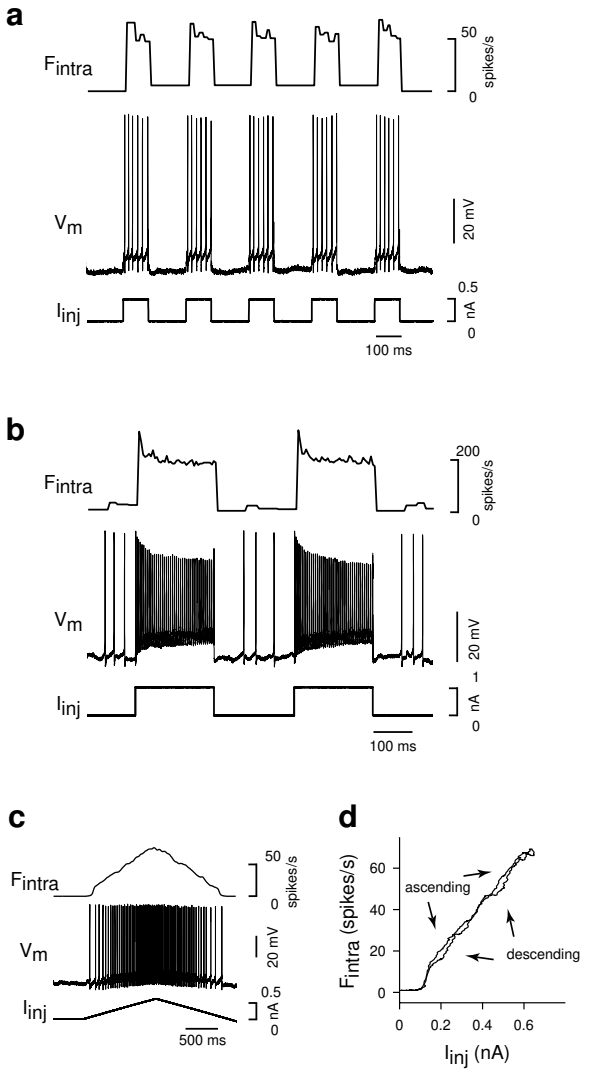

Fig. 5. Transient depolarizing current injection during single fixations did not induce persistent increase of discharge rate or membrane potential. (a) Change in firing rate and membrane potential in response to intracellular depolarizing current injection during a nasal fixation. (b) Change in firing rate and membrane potential in response positive current injection during a fixation above position threshold. (c) Firing rate and membrane potential in response to a depolarizing triangular current pulse during a nasal fixation. (d) Firing rate plotted against injected current for the ramps in (c).

aged 30.2 ± 16.3 MΩ (range, 17–55 MΩ; $n = 6$). When deeply hyperpolarized with current injection ($-80 > V_m > -100$ mV), impedance dropped to 9.5 ± 2 MΩ ($n = 2$). When neurons were depolarized to slightly above rest with current injection (~5 mV), apparent input impedance, measured with hyperpolarizing current steps (< 0.5 nA) that blocked all discharge, averaged 12.5 ± 3.5 MΩ ($n = 2$).

We assessed membrane relaxation time following small current steps (< 0.5 nA) in the absence of discharge while neurons were at rest or slightly hyperpolarized (5–10 mV). Relaxation time was estimated by determining the point at which the post-stimulus potential returned two-thirds of the way to the pre-stimulus level. This value averaged 16.3 ± 3.9 ms (range, 12–21.5 ms; $n = 5$).

Position-associated membrane potential fluctuations

If position neurons receive excitatory feedback from each other, then changes in tonic firing should be accompanied by changes in the rate of excitatory postsynaptic potentials (EPSPs). Alternatively, changes in tonic firing could result from changes in the amplitude of incident PSPs from neurons with constant rates. In practice, it can be difficult to resolve individual PSPs *in vivo* because of their high rates and passive filtering by dendritic cables. Therefore, we relied on the variance of membrane potential[30] as an indirect measure of changes in the rate or amplitude of synaptic input.

Interspike membrane potential accompanying fixations showed pronounced fluctuations throughout the recording (I_{inj}, 0 to –1 nA). Two examples from cells exhibiting prominent fluctuations are shown in Fig. 7a and b, in which insets highlight increased fluctuation amplitude at temporal eye positions. In 15 recordings, firing rate was low enough so that fluctuations during segments of interspike membrane potential could be compared at different fixations. Fluctuations were quantified over a complete cycle of the scanning pattern. Root mean square interspike membrane potential (V_{is}^{rms}) values for each fixation were determined by averaging over 30-ms interspike segments within each fixation (see Methods). For the population of cells analyzed, mean V_{is}^{rms} was 0.49 ± 0.19 mV ($n = 15$). In 4 of 15 cells, V_{is}^{rms} significantly increased with temporal position, and with V_{is} ($r > 0.8$; slope, 50 ± 20 μV/mV; $p < 0.05$; **Fig. 7a**, **b** and **c**). Correlation between V_{is}^{rms} and V_{is} was not observed in the other position neurons ($p > 0.05$).

To explore the origin of fluctuation changes, we suppressed action potentials with hyperpolarization (**Fig. 7d**; $n = 8$, including 3 that showed correlation between V_{is}^{rms} and V_{is}), which allowed assessment of fluctuations in the absence of any after-polarizations. Fluctuations were quantified over a complete cycle of the scanning pattern, with root mean square membrane potential (V_m^{rms}) measured using 100-ms segments. In two of eight cells, V_m^{rms} significantly increased with temporal position, and with V_m ($r > 0.8$; slope, 100 ± 40 μV/mV, $p < 0.01$). Correlation between V_m^{rms} and V_m was not observed in the other position neurons ($p > 0.05$). The two neurons that did show correlation were of the set of three neurons whose V_{is}^{rms} and V_{is} were correlated.

The observed variations in fluctuation amplitude are consistent with a change in synaptic activity with fixation position. However, the position dependence of fluctuations may have been caused simply by voltage dependence of intrinsic currents. To explore this possibility, one of these two position neurons was injected with a train of brief current steps during transitions between nasal and temporal fixations (**Fig. 7d**). Despite significant electrode-generated change in membrane potential (~10 mV), little change of fluctuation characteristics occurred within a fixation. The fluctuations during the temporal fixation were still larger in amplitude than during the nasal fixation, even when the membrane potential was more hyperpolarized during the temporal fixation (**Fig. 7d**).

This observation was quantified for 10 fixation transitions. Direct comparison of the difference in V_m^{rms} between fixations (ΔV_m^{rms}) was made for two different data sets: first, a set with I_{inj} equal to –0.3 nA during both fixations, and second, a set with I_{inj} equal to –0.3 nA during the nasal fixation and –1.0 nA during the temporal one. For both data sets, ΔV_m^{rms} was plotted against change in average membrane potential between temporal and nasal fixations, with I_{inj} equal to –0.3 nA (set 1, **Fig. 7e**, top; set 2, **Fig. 7e**, bottom). For both sets, V_m^{rms} was consistently higher at temporal positions (set 1, $\Delta V_m^{rms}/\Delta V_m = 40 \pm 20$ μV/mV, $p < 0.001$;

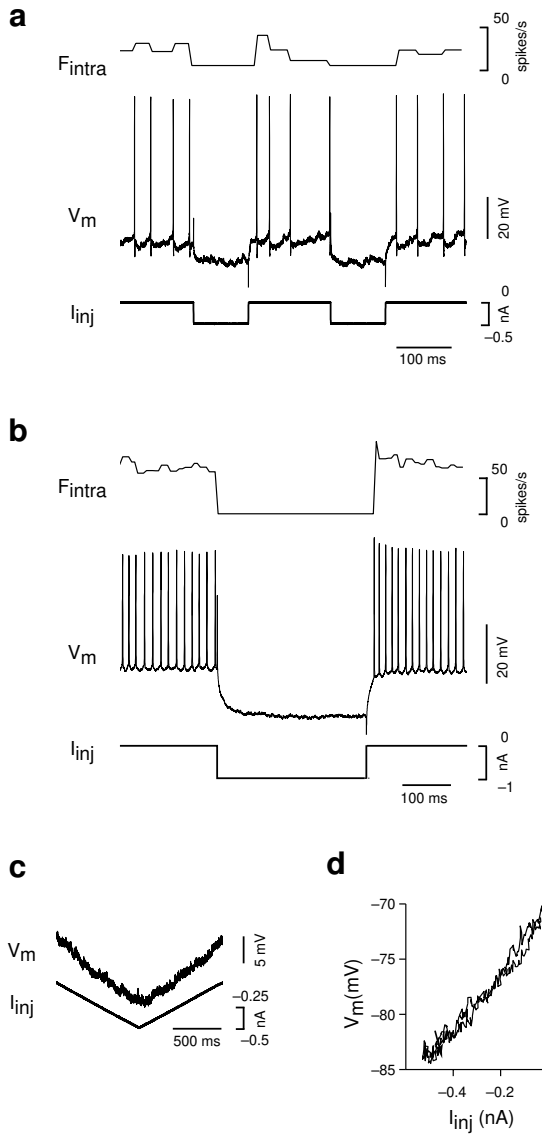

Fig. 6. Transient hyperpolarizing current injection during single fixations did not induce persistent decrease of discharge rate or membrane potential. (a) Change in firing rate and membrane potential in response to intracellular hyperpolarizing current injection during a fixation above position threshold. (b) Changes during large amplitude, long duration perturbations. (c) Membrane potential in response to a hyperpolarizing triangular current pulse during a nasal fixation. (d) Membrane potential plotted against injected current for the ramps in (c).

set 2, $\Delta V_m^{rms}/\Delta V_m = 80 \pm 40$ μV/mV, $p < 0.001$; $n = 10$ fixation transitions). This result demonstrates that the fluctuation changes during spontaneous eye movements cannot be explained by the voltage dependence of intrinsic currents.

Discussion

These results provide information about persistent activity that was previously unattainable by analysis of extracellular recordings. A basic finding was that brief current injections producing artificial saccade-like changes in firing rate did not produce persistent changes in neural activity. A second finding was that steps in firing rate and fixation were accompanied by pronounced steps in membrane potential. Finally, in a quarter of the recordings, nasal to temporal steps in ipsilateral eye position were accompanied by increased root mean square (RMS) fluctuation of membrane potential.

Single-cell stimulation and induction of persistence

Intracellular injection of current did not generate sustained plateau potentials or terminate membrane potential steps produced during spontaneous eye movements. In addition, the application of repeated steps in close succession failed to elicit any systematic increase in firing rate, indicating the absence of a slow buildup in rate, termed 'windup,' that has been observed in motoneurons[31]. These results suggest that plateau potentials are not involved in the generation of persistent neural activity in position neurons. There are, however, several caveats. Because intracellular recordings were probably close to the soma[11] and distal dendrites commonly extend five hundred microns[11], dendritic cable attenuation may have isolated putative distal plateau potentials from perturbation. However, when we replaced potassium with cesium as the recording solution cation to decrease the electrotonic length of the cell, we were still unable to alter membrane potential steps. Plateau potentials may also have been transiently altered by injected current, only to be rapidly re-initiated by synaptic currents when injected current was turned off.

Continuous high-frequency extracellular stimulation of regions near putative VPNI sites produce ipsilaterally directed drift of the eyes over tens of degrees and fast phases that reset eye position[32,33]. The slow drift has a roughly constant velocity, consistent with temporal integration of a constant amplitude stimulus. Why, then, does extracellular activation of many neurons, but not a single-cell, seem to be integrated? One possibility is that the single cell stimulation had a weak effect on the VPNI that may be detectable only by signal averaging of hundreds or thousands of trials. Other possibilities are that single-cell stimulation did not surpass a stimulus threshold or activate critical synaptic inputs to the integrator. Short-term potentiation of synaptic inputs carrying eye velocity signals has been proposed as a mechanism for oculomotor integration[34]. This mechanism predicts no persistent change following transient change of firing rate in position neurons, consistent with our data.

Membrane potential steps during eye movements

Analysis of extracellular spike waveforms previously led to the suggestion that area I position neuron dendrites support sodium spike propagation[11]. Such dendritic spikes could provide a cellular positive feedback mechanism by providing depolarization necessary for voltage-dependent currents such as those of the NMDA receptor[35]. The results presented here, demonstrating that steps in membrane potential remained when sodium action potential initiation was blocked by hyperpolarizing current injection, suggest that spike-based depolarization of the dendrites is not necessary for the generation of step changes in membrane potential.

Two other cellular mechanisms for persistent neural activity were rendered unlikely by our experiments: persistent changes in subthreshold pacemaker currents, and persistent changes in action potential threshold. None of our recordings showed evidence of subthreshold pacemaker currents, whereas action potential threshold increased, rather than decreased, during steps with higher firing rates.

Membrane potential fluctuations

A clear increase in RMS fluctuation of membrane voltage was observed during more depolarized steps. The conceptual frame-

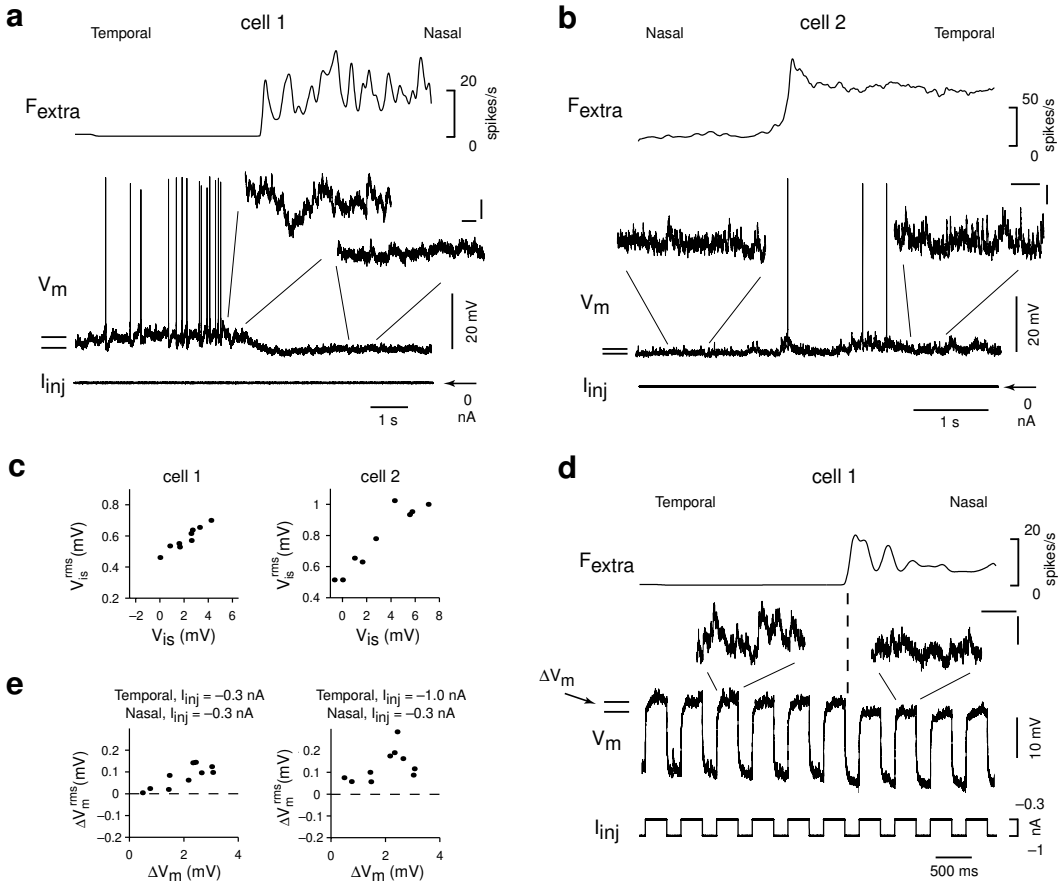

Fig. 7. Persistent changes in the amplitude of membrane potential fluctuations correlated with steps in membrane potential. (**a**, **b**) Membrane potential change during fixation transition accompanied by change in the amplitude of membrane potential fluctuations (insets). In (**a**), fixation position was monitored by the activity of a contralateral abducens motoneuron; a step increase of firing rate (F_{extra}) was correlated with a step decrease in membrane potential. In (**b**), fixation position was monitored by the activity of a second ipsilateral position neuron. Scale bars, 50 ms and 2 mV. (**c**) Root mean square interspike membrane potential (V_{is}^{rms}) plotted against membrane potential for two position neurons. (**d**) Membrane potential changes for the position neuron in (**a**) during suppression of action potential discharge. Transitions in fixation position (dashed line) were still accompanied by changes in fluctuation amplitude (insets). Different levels of hyperpolarizing current were used to investigate the voltage dependence of changes in fluctuation amplitude (see results). Scale bars, 50 ms and 2 mV. (**e**) Quantitation of change in the amplitude of membrane potential fluctuations during action potential suppression. ΔV_m is the difference in membrane potential between fixations with I_{inj} equal to –0.3 nA, as indicated in (**d**).

work developed[30] for the study of increased membrane potential fluctuations at the neuromuscular junction during depolarization induced by acetylcholine may be applicable to understanding our results. Increased fluctuations were attributed to an increased rate of single molecule binding events: if the binding of an acetylcholine molecule produces a 'shot effect' transient depolarization, then an increased rate of binding during acetylcholine application would lead to both increased mean membrane potential and increased membrane potential variance. Here we found increased fluctuations at temporal fixation positions (**Fig. 7**). By analogy, this increased fluctuation amplitude could reflect an increased rate of EPSPs. Because the discharge rates of other position neurons were also increasing with temporal fixation position, the fluctuations observed were consistent with excitatory recurrent feedback within the VPNI. However increased synchrony of synaptic inputs, rather than simply increased rate of synaptic events, could also lead to increased membrane potential noise[36]. In addition, increased RMS noise could be produced by a change in the amplitude of synaptic events with no change in rate. Position neurons modulate their firing rates during horizontal VOR, implying that they receive tonic inputs from neurons carrying head velocity signals. Saccadic inputs may alter the amplitude of these tonic inputs, leading to a change in mean membrane potential and RMS noise. Experiments that resolve single postsynaptic currents could differentiate between these possibilities.

Only a quarter of the recordings analyzed exhibited significant correlation between RMS fluctuation noise and mean membrane potential. This ratio may simply reflect the probability that a recording site was close enough to dendritic regions that received synaptic inputs modulated with eye position.

Other implications for recurrent network models

We found an approximately linear relationship between firing rate and injected current (**Fig. 5c** and **d**). This supports the use of model neurons having this property in recurrent network models of the VPNI[24]. The observation of multiple-component slow

AHPs following action potentials is consistent with a possible involvement of slow potassium currents in the generation of a linear relationship between firing rate and injected current[27,28].

In existing network VPNI models[14,21–24], the persistence of activity in a single neuron is characterized by a cellular time constant; tuned positive feedback through recurrent synapses boosts the time constant of persistent activity in the network above that of the single cell. In general, longer cellular time constants reduce the precision required in tuning feedback[24]. If the apparent 15-ms membrane time constant we measured in VPNI neurons determines the relevant cellular time scale for integration in area I, then feedback tuning requirements would be very stringent. Therefore, it may be important to look for slower cellular processes that could reduce the precision required, such as short-term synaptic plasticity or slowly decaying synaptic conductances, as well as mechanisms for adaptively tuning feedback based on VPNI performance.

METHODS

Preparation and electrophysiology. All experiments were done in compliance with the Guide for the Care and Use of Laboratory Animals (http://www.nap.edu/readingroom/books/labrats). Specific protocols were approved by the Institutional Animal Care and Use Committee. Goldfish (*Carassius auratus*, 3–5 inches from tip to peduncle, 25–50 g) were purchased from a commercial supplier (Hunting Creek Fisheries, Thurmont, Maryland) and kept at 20–22°C in a 50-gallon aquarium with daily exposure to light. The methods used for head restraint, surgical preparation, recording of extracellular action potentials, area I mapping, and eye movement measurements were as described previously[11].

Intracellular recordings from neurons in area I were obtained with sharp electrodes or patch electrodes in the current-clamp configuration. Sharp electrodes filled with recording solution (1 M KCl, 50 mM KH_2PO_4, 1 mM Fast Green, pH 7.4) were beveled to a resistance of 60–120 MΩ. In five analyzed recordings, 1–2% Neurobiotin was added to the recording solution to visualize cell morphology[11]; in two other analyzed cases, cesium was substituted for potassium. Sharp electrodes were aimed toward the somata and proximal dendrites of position neurons[11]. Patch electrodes (bubble #4.5–5) were filled with intracellular solution (115 mM K-methanesulfonate, 9.6 mM K-HEPES, 3 mM Na_2-ATP, 1 mM Fast Green, 0.3 mM Na_3-GTP, 0.3 mM $MgCl_2$, 0.1 mM K_2-EGTA, pH 7.3 with KOH, 252 mOsm) and had a resistance of 6–10 MΩ. Patch electrodes were kept free of debris during penetration to area I by application of 1 psi positive pressure; once within area I, backing pressure was reduced to 0.1–0.2 psi to enable a search for increases in resistance indicative of proximity to a neuron. Intracellular voltage signals were low-pass filtered (5 kHz, 12 pole-Bessel, Cygnus Technologies, Delaware Water Gap, Pennsylvania) and digitally sampled at rates of at least 10.00 kHz on a Digidata 1200B data acquisition system and Clampex 7.0 software (Axon Instruments, Foster City, California). Saccadic and fixation behavior was assessed directly by monitoring eye movements with the scleral search-coil method[11,37]. In 12 of 18 preparations from which analyzed recordings of position neurons were obtained, 40 μg gallamine triethiodide (Flaxedil, American Cyanamid, Wayne, New Jersey) or 1 μg doxacurium chloride (Nuromax, Glaxo Wellcome, Research Triangle Park, North Carolina) was intramuscularly injected to afford increased stability of recording. In these situations, eye movements were still present, but attenuated to the extent that fixation behavior was better monitored by using the firing rates of neurons correlated with horizontal eye position. This latter measurement of 'fictive eye movements' was done with a second extracellular recording microelectrode positioned in either the abducens nucleus[38] or area I. Combined intracellular and extracellular recordings were obtained by establishing the extracellular recording first. Intracellular recordings were maintained for a median time of 5 min (range, 1–60 min).

Analysis. Neurons exhibiting step-like variation in firing rate (I_{inj}, 0 to –1 nA) like that in Fig. 1a were selected for further analysis as position neurons (n = 18 total; n = 15 sharp, n = 3 patch). At least one full cycle was analyzed for each cell. In seven of these recordings, fixation behavior was independently monitored by extracellular neural recording, and in three others, by the scleral search-coil method. Each analyzed cell was recorded in a different preparation. All data were analyzed in the Matlab environment (MathWorks, Natick, Massachusetts).

Saccades were determined by identifying rapid (< 0.2 s) and large transitions in either eye position (> 2°) or firing rate (> 5 spikes/s). Cells were identified as exhibiting saccade-related bursts or undershoots of rate as previously described[11]; cells were identified as exhibiting transient depolarizations if overshooting membrane potential deviations that were more than 1 mV above the subsequent post-saccadic potential were observed on 75% of saccades. Interspike membrane potential during periods of discharge was measured after removal of data segments that began 1 ms before and ended 3 ms after the peak of an action potential. This procedure removed all supra-threshold activity and part of the after-hyperpolarization, which in some recordings, could last approximately 40 ms. Average fixation parameters were calculated over a region that began 150 ms after a saccade and ended 150 ms before the next saccade. In Figs. 2, 4 and 7, average potential indicators to the left of traces are calculated over entire fixations using these conditions, and not just the regions shown. Firing rate was calculated by a previously described method using a smoothing window of 150 ms (ref. 11) except when brief current pulses (**Figs. 5** and **6**) were applied, in which case rate was calculated by finding the reciprocal of the interspike interval. Apparent action potential threshold within a fixation was determined using an action potential profile found by averaging the waveforms of the first 10 spikes in the fixation. A cycle of the scanning pattern used for assessment of the relationship between average firing rate and membrane potential included fixations immediately below position threshold when present. All tests for assessing the significance of correlations were done using a one-tailed t-test. All values given with a ± indicator represent mean ± s.d..

All analyzed responses to injected current pulses were from regions of data that did not include saccadic transitions. Injections applied above the position threshold were done without reference to the nasal–temporal degree of fixation position. Bridge-balance was normally maintained during the recording with the use of small (<0.3 nA) test pulses; remaining imbalance was corrected during analysis by using as a reference the peak height of action potentials before injection. The sensitivity g_{inj} was assessed using 2–10 data points of firing rate and membrane potential evoked by injected current pulses or ramps that varied in length from 0.2–2.0 s and did not overlap with saccades. Furthermore, measurements were made only for variations in induced firing rate that were similar to the variations observed during assessment of the sensitivity g_{spont}. Persistent effects of transient current injection were assessed using 5–10 injection pulses per cell for each polarization direction. The firing rate before, during and after injection pulses was measured over identical length windows that were 0.15–0.5 s long. Changes in intracellular firing rate (ΔF_{intra}) were defined as post-step minus pre-step firing rate.

Root mean square (RMS) analysis was done by first breaking membrane potential records during fixations into segments that were either 30 or 100 ms long (see Results). If the fixation period was accompanied by discharge, each segment was contained within a single interspike region. If membrane potential transitioned between two polarizations because of direct current injection, the initial 50 ms after a current step was not used. Next, 'slope-subtraction' was done by calculating a best fit line (in the least-squares sense) to the data segment and subtracting the ordinate values of this line. The RMS value for a given fixation was calculated as the mean RMS of all segments taken from that fixation.

ACKNOWLEDGEMENTS

We thank G. Major and F. Helmchen for comments on the manuscript.

RECEIVED 21 SEPTEMBER; ACCEPTED 18 DECEMBER 2000

1. Fuster, J. M. & Alexander, G. E. Neuron activity related to short-term memory. *Science* **173**, 652–173 (1971).
2. Fuster, J. M. *Memory in the Cerebral Cortex* (MIT Press, Cambridge, Massachusetts, 1995).
3. Goldman-Rakic, P. S. Cellular basis of working memory. *Neuron* **14**, 477–485 (1995).

4. Schultz, W. & Romo, R. Role of primate basal ganglia and frontal cortex in the internal generation of movements. I. Preparatory activity in the anterior striatum. *Exp. Brain. Res.* **91**, 363–384 (1992).
5. McFarland, J. L. & Fuchs, A. F. Discharge patterns in nucleus prepositus hypoglossi and adjacent medial vestibular nucleus during horizontal eye movement in behaving macaques. *J. Neurophysiol.* **68**, 319–332 (1992).
6. Lopez-Barneo, J., Darlot, C., Berthoz, A. & Baker, R. Neuronal activity in prepositus nucleus correlated with eye movement in the alert cat. *J. Neurophysiol.* **47**, 329–352 (1982).
7. Pastor, A. M., de la Cruz, R. R. & Baker, R. Eye position and eye velocity integrators reside in separate brainstem nuclei. *Proc. Natl. Acad. Sci. USA* **91**, 807–811 (1994).
8. Prut, Y. & Fetz, E. E. Primate spinal interneurons show pre-movement instructed delay activity. *Nature* **401**, 590–594 (1999).
9. Robinson, D. A. Integrating with neurons. *Annu. Rev. Neurosci.* **12**, 33–45 (1989).
10. Easter, S. S. Spontaneous eye movements in the goldfish. *Vision Res.* **11**, 333–342 (1971).
11. Aksay, E., Baker, R., Seung, H. S. & Tank, D. W. Anatomy and discharge properties of pre-motor neurons in the goldfish medulla that have eye-position signals during fixations. *J. Neurophysiol.* **84**, 1035–1049 (2000).
12. Skavenski, A. A. & Robinson, D. A. Role of abducens neurons in vestibuloocular reflex. *J. Neurophysiol.* **36**, 724–738 (1973).
13. Robinson, D. A. in *Handbook of Physiology* (eds. Brookhart, J. M. & Mountcastle, V. B.) 1275–1320 (American Physiology Society, Bethesda, Maryland, 1981).
14. Seung, H. S. How the brain keeps the eyes still. *Proc. Natl. Acad. Sci. USA* **93**, 13339–13344 (1996).
15. Keller, E. L. & Robinson, D. A. Absence of a stretch reflex in extraocular muscles of the monkey. *J. Neurophysiol.* **34**, 908–919 (1971).
16. Hounsgaard, J., Hultborn, H., Jesperen, B. & Kiehn, O. Bistability of α-motoneurons in the decerebrate cat and in the acute spinal cat after intravenous 5-hydroxytryptophan. *J. Physiol. (Lond.)* **405**, 345–367 (1988).
17. Kiehn, O. Plateau potential and active integration in the 'final common pathway' for motor behavior. *Trends Neurosci.* **14**, 68–73 (1991).
18. Reuveni, I., Friedman, A., Amitai, Y. & Gutnick, M. J. Stepwise repolarization from Ca^{2+} plateaus in neocortical pyramidal cells: evidence for nonhomogenous distribution of HVA Ca^{2+} channels in dendrites. *J. Neurosci.* **13**, 4609–4621 (1993).
19. Marder, E., Abbott, L. F., Turrigiano, G. G., Liu, Z. & Golowasch, J. Memory from the dynamics of intrinsic membrane currents. *Proc. Natl. Acad. Sci. USA* **93**, 13481–13486 (1996).
20. Catterall, W. A. Molecular properties of brain sodium channels: an important target for anticonvulsant drugs. *Adv. Neurol.* **79**, 441–456 (1999).
21. Kamath, B. Y. & Keller, E. L. A neurological integrator for the oculomotor control system. *Math. Biosci.* **30**, 341–352 (1976).
22. Rosen, M. J. A theoretical neural integrator. *IEEE Trans. Biomed. Eng.* **19**, 362–367 (1972).
23. Cannon, S. C., Robinson, D. A. & Shamma, S. A proposed neural network for the integrator of the oculomotor system. *Biol. Cybern.* **49**, 127–136 (1983).
24. Seung, H. S., Lee, D. D., Reis, B. Y. & Tank, D. W. Stability of the memory of eye position in a recurrent network of conductance-based model neurons. *Neuron* **26**, 259–271 (2000).
25. Llinás, R. R. & Yarom, Y. Oscillatory properties of guinea-pig inferior olivary neurones and their pharmacological modulation: an in vitro study. *J. Physiol. (Lond.)* **376**, 163–182 (1986).
26. Amitai, Y. Membrane potential oscillations underlying firing patterns in neocortical neurons. *Neuroscience* **63**, 151–161 (1994).
27. Wang, X. J. Calcium coding and adaptive temporal computation in cortical pyramidal neurons. *J. Neurophysiol.* **79**, 1549–1566 (1998).
28. Ermentrout, B. Linearization of F-I curves by adaptation. *Neural Comput.* **10**, 1721–1729 (1998).
29. Kiehn, O. & Eken, T. Functional role of plateau potentials in vertebrate motor neurons. *Curr. Opin. Neurobiol.* **8**, 746–752 (1998).
30. Katz, B. & Miledi, R. The characteristics of 'end-plate noise' produced by different depolarizing drugs. *J. Physiol. (Lond.)* **230**, 707–717 (1973).
31. Perrier, J.-F. & Hounsgaard, J. Ca (2+)-activated nonselective cationic current (I(CAN)) in turtle motoneurons. *J. Neurophysiol.* **82**, 730–735 (1999).
32. Cannon, S. C. & Robinson, D. A. Loss of the neural integrator of the oculomotor system from brain stem lesions in monkey. *J. Neurophysiol.* **57**, 1383–1409 (1987).
33. Godaux, E., Cheron, G. & Gravis, F. Eye movements evoked by microstimulations in the brainstem of the alert cat. *Exp. Brain Res.* **77**, 94–102 (1989).
34. Shen, L. Neural integration by short term potentiation. *Biol. Cybern.* **61**, 319–325 (1989).
35. Yuste, R. & Denk, W. Dendritic spines as basic functional units of neuronal integration. *Nature* **375**, 682–684 (1995).
36. Destexhe, A. & Pare, D. Impact of network activity on the integrative properties of neocortical pyramidal neurons in vivo. *J. Neurophysiol.* **81**, 1531–1547 (1999).
37. Robinson, D. A. A method of measuring eye movement using a scleral search coil in a magnetic field. *IEEE Trans. Biomed. Electron.* **10**, 137–145 (1963).
38. Pastor, A. M., Torres, B., Delgado-Garcia, J. M. & Baker, R. Discharge characteristics of medial rectus and abducens motoneurons in the goldfish. *J. Neurophysiol.* **66**, 2125–2140 (1991).